

INTERNATIONAL SOCIETY FOR SOIL MECHANICS AND GEOTECHNICAL ENGINEERING



This paper was downloaded from the Online Library of the International Society for Soil Mechanics and Geotechnical Engineering (ISSMGE). The library is available here:

<https://www.issmge.org/publications/online-library>

This is an open-access database that archives thousands of papers published under the Auspices of the ISSMGE and maintained by the Innovation and Development Committee of ISSMGE.

Cavity effect on collapse load of strip footings

Effect de cavité sur le chargement effondre de fondation de bande

M.C.Wang — Prof., Dept. of Civil Engineering, The Pennsylvania State University, University Park, PA 16802, USA
Young-Uk Kim — Post Doctoral Research Fellow, Dept. of Civil Engineering, Korea University, Seoul, Korea
Jin-Taek Jun — Engineer, Patel Chen Associates, Inc., P.O. Box 287, 9916 Allentown Blvd, Grantville, PA 17028, USA

ABSTRACT: The effect of continuous circular cavities on the collapse load of overlying strip surface footings was investigated using the upper bound theorem of limit analysis. The analysis was made for a range of footing size, cavity size, and soil property. Ten collapse mechanisms were analyzed. The smallest collapse footing pressure obtained from these ten collapse mechanisms was taken as the ultimate bearing capacity of the footing. Based on the results of analysis, correlation equations and figures were developed. These equations and figures can be used to determine the influence zone, the critical depth to cavity, and the ultimate bearing capacity of a strip footing underlain by a cavity.

RÉSUMÉ: L'effet de cavités circulaires continues sur le chargement d'effondrement de fondations de surface de bande sus-tendue a été examiné utilisant le théorème de limite supérieur d'analyse de limite. L'analyse a été faite pour une portée de fondation de taille, la taille de cavité, et la propriété de sol. Dix mécanismes d'effondrement ont été analysés. La plus petite pression de fondation d'effondrement obtenue de ces dix mécanismes d'effondrement a été prise comme la capacité ultime qui soutient les fondations. Basé sur les résultats d'analyse, d'équations de corrélation et de figures ont été développées. Ces équations et les figures peuvent être utilisées pour déterminer la zone d'influence, la profondeur critique de la cavité, et la capacité ultime -qui soutient- d'une bande sous-tendue par une cavité.

1 INTRODUCTION

Underground cavities can be either naturally formed, e.g. solution cavities in soluble rocks, or man-made, e.g. tunnels or mine cavities. When cavities are near footings, they may interact with each other resulting in an adverse effect of the cavity on the footing performance. Numerous studies related to this subject matter are available; some of the studies deal with cavity-footing interaction, e.g. Badie & Wang (1994), and Yoo & Wang (1994), while others with cavity effect on footing stability, e.g. Baus & Wang (1983), Wood & Lamach (1985), Badie & Wang (1984, 1985), and Abdellah & Ablalla (1987). There are also studies concerning the determination of bearing capacity of footings above cavities, e.g. Wang & Hsieh (1987), and Hsieh & Wang (1992). All of these studies provide fundamental bases for the development of a generally accepted methodology for analysis and design of footings underlain by cavities. An essential element in the design methodology is the method for determination of bearing capacity under varying conditions of cavity, footing, loading, and soil property. The available methods for the determination of bearing capacity are developed only for limited cavity and soil conditions. To develop a method that can consider a broader range of conditions, a study was undertaken using the upper bound theorem of limit analysis. The results of the study including ultimate bearing capacity as well as charts, which delineate influence zones and contours of equal percentage of bearing capacity are presented herein.

2 FORMULATION

The analysis is made using the upper bound theorem of limit analysis for strip footings overlying and parallel with continuous circular cavities. The footing having a width of B is rigid and is subjected to a vertical central load. The circular cavity having a diameter of W is located at a depth of D (vertical distance between footing base and cavity top) with an eccentricity of E (horizontal distance between footing and cavity centers). The supporting soil behaves as a rigid-plastic material that can be characterized by c (cohesion) and ϕ (internal friction angle). In the analysis of collapse footing pressure, ten collapse mecha-

nisms were considered. These mechanisms were conjectured based on the available information on the failure surfaces observed from the finite element analysis and the model footing

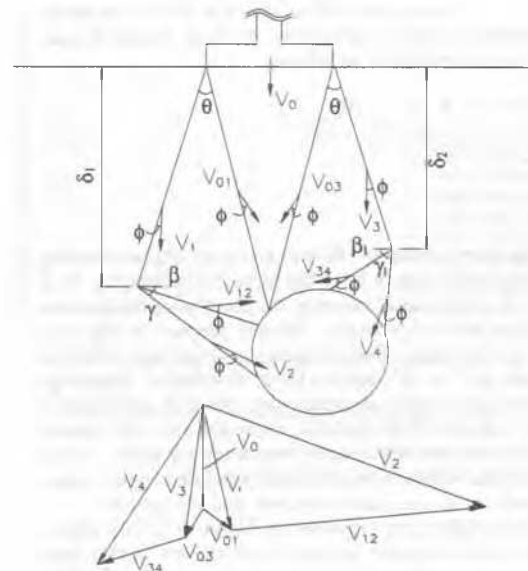


Fig.1 Failure Mechanism and Hodographs

tests of Baus (1980), Badie (1983), and others. One of the ten collapse mechanisms together with hodographs is illustrated in Figure 1. For each collapse mechanism, the rate of energy dissipation along the slip lines and the rate of work done by footing pressure, soil weight, and fluid pressure inside the cavity, if any, were obtained. By equating the rate of energy dissipated to the rate of work done, the equation for collapse footing pressure as a function of footing size, cavity size and location, and soil property was formulated. Each equation contained one or more variables that define the geometry of the collapse mechanism.

3 COMPUTER ANALYSIS

To obtain the collapse footing pressure, the footing pressure in each equation needs to be minimized with respect to the variables. Because of the complexity of the equations, it is very difficult, if not impossible, to present the minimized equation in a simple form. Therefore, the minimization was performed on a PC. In addition to the computer analysis for footings above cavities, the collapse footing pressures of footings without cavities (no-cavity condition) was also computed from Hill's mechanism (Chen, 1974).

4 RESULTS OF ANALYSIS

The collapse footing pressures for footings above cavities are expressed as a percentage of no-cavity condition, and are related with D/B for different W/B and E/B values. The lowest value of collapse footing pressure determined from the various collapse mechanisms is taken as the ultimate bearing capacity of the footing. The results of analysis show, as would be expected, that the ultimate bearing capacity increases with increasing D/B to a depth beyond which it becomes a constant value. This depth to cavity is termed the critical depth (Baus & Wang, 1983), since below this depth, the ultimate bearing capacity remains at 100% indicating no effect of cavity on footing stability. Note that due to space limitation, no data are presented herein. When the cavity is located above the critical depth, the footing stability will be adversely influenced by the cavity. Thus, the zone between footing base and critical depth can be termed as the influence zone. From the graphs, which relate the ultimate bearing capacity and D/B, the influence zone for different W/B can be generated. In addition, within the influence zone, contours of equal percentage of no-cavity ultimate bearing capacity can be obtained. Figure 2 presents such a graph for W/B=3.0 with $c=158.6 \text{ kN/m}^2$, $\phi=8^\circ$, and $\gamma=16.5 \text{ kN/m}^3$.

The influence zone graphs are further modified to take into account the soil property. The modified graphs are shown in figures 3(A), (B), and (C) for 100%, 75% and 50% of no-cavity ultimate bearing capacity, respectively. In these figures, the parameters η and λ are defined as follows;

$$\eta = \frac{D}{W} \cdot \left(\frac{1+W/B}{2} - \frac{W/B}{10} \right) \cdot \left(\frac{50^\circ}{\phi^\circ + 50^\circ} \right) \cdot \lambda \quad (1)$$

$$\lambda = \frac{c}{\gamma \cdot B} \quad (2)$$

Note that when applied to 100% of no-cavity ultimate bearing capacity contours in Figure 3(A), the term D becomes D_{cr} . It is seen that η is a function of not only the depth to cavity but also the cavity size and soil property. The soil property is also considered in λ . The range of soil property analyzed are $c=23.9$ to 143.6 kN/m^2 , $\phi=5^\circ$ to 35° , and $\gamma=15.7$ to 20.4 kN/m^3 . Both Figures 3(B) and (C) contain two zones; the zone with solid lines is valid for all values of W/B analyzed, while the zone with dashed lines is valid only for W/B greater than a certain value. These three figures can be used to estimate the ultimate bearing capacity for a given cavity size, cavity location, and soil property.

The critical depth data presented in Figure 3(A) and others, which have been computed but not presented, are further integrated in Figure 4. Figure 4 relates parameters η with λ for a constant E/B; three values of E/B, i.e. 0, 1.5, and 3.0, are presented. Along each graphical relation are shown data points obtained for different internal friction angles of 5° , 15° , and 35° . The data points fluctuate along the line in a narrow range without a definite pattern, suggesting that the internal friction angle have little effect on the correlation. The regression analysis of the data shows the following relations:

$$\eta = 1.60 + 3.91\lambda \quad \text{for } E/B=0 \quad (3)$$

$$\eta = 3.31 + 2.35\lambda \quad \text{for } E/B=1.5 \quad (4)$$

$$\eta = 2.68 + 1.56\lambda \quad \text{for } E/B=3.0 \quad (5)$$

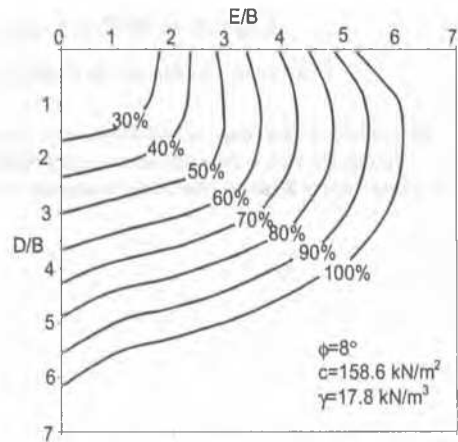


Fig.2 Contours of Equal Percentage of No-Void Ultimate Bearing Capacity for W/B=3.0

For the correlation equations, the adjusted R-square values are 0.986, 0.985 and 0.986, and p-values are 0.0052, 0.00055 and 0.0043 for E/B=0, 1.5, and 3.0, respectively. These regression parameters indicate a very good fit of the equations to the data points. Equations (3), (4), and (5) were developed from 100% of no-cavity ultimate bearing capacity data. Therefore, in the η definition, i.e. Equation (1), the depth to void (D) should be replaced by critical depth (D_{cr}). From these equations, i.e. Equations (1) through (5), the critical depth to void can be determined for a given soil property and void size.

5 DISCUSSIONS

To determine the critical depth using Equations (3), (4), or (5), the value of parameter λ must be computed first. The value of λ is entered in Equations (3), (4), or (5) to find η . Then, D_{cr} is computed for the given values of W, B, and ϕ using Equation (1). When E/B value is different from 0, 1.5 and 3.0, the method of interpolation is needed. The critical depth data thus obtained are plotted against the available data of Baus & Wang (1987), Badie & Wang (1985), and Hsieh & Wang (1987) in Figure 5. Also included in the figure is a 45°-line. Note that the available data were obtained from the results of finite element analysis, which characterized the foundation soil as an elasto-plastic material. The upper bound theorem of limit analysis adopted in this study characterized the soil as a rigid-plastic material as stated earlier. The data presented in Figure 5 are generated from three soils – a kaolin ($c=158.5 \text{ kN/m}^2$ and $\phi=8^\circ$), a silty clay ($c=65.5 \text{ kN/m}^2$ and $\phi=13.5^\circ$) and a clayey sand ($c=9.2 \text{ kN/m}^2$ and $\phi=31^\circ$).

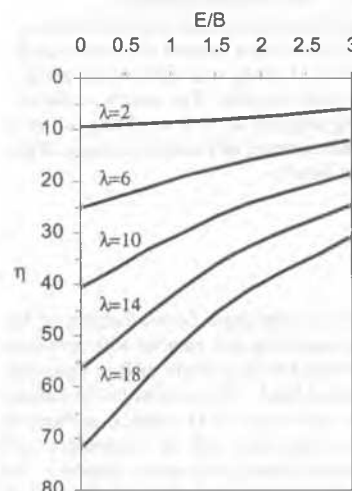


Fig.3 (A) Contours of 100% No-Void Ultimate Bearing Capacity

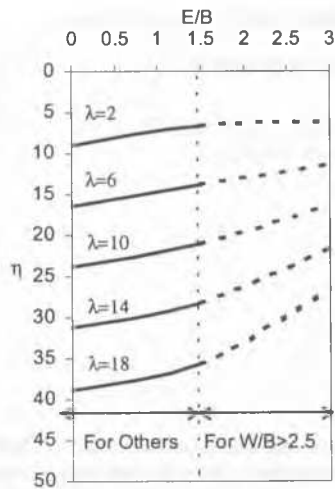


Fig.3(B) Contours of 75% No-Void Ultimate Bearing Capacity

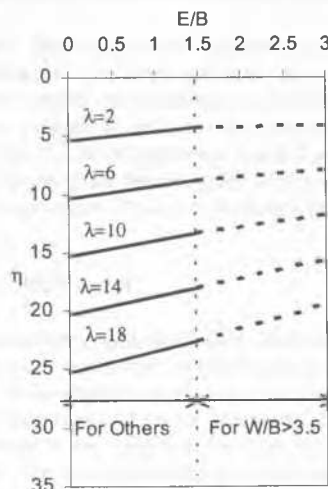


Fig.3(C) Contours of 50% No-Void Ultimate Bearing Capacity

This figure shows that, except for four data points – two dotted triangles and two dotted circles, which are farther away from the 45°-line, the agreement between the two sets of data, generally speaking, is fairly good. These four outliers are obtained from the clayey sand. It is also seen that all of the data points of the clayey sand are located above the 45°-line. This may suggest that the clayey sand may not be best characterized as a rigid-plastic material in the limit analysis. While Figure 2 represents the critical depth contour (100% curve), it also contains contours of equal percentage of no-cavity ultimate bearing capacity for a given soil property with $W/B=3.0$. For other void sizes, void locations, and soil properties, the ultimate bearing capacity can be estimated from Figures 3(A), 3(B), and 3(C), as mentioned earlier. In applications, it should be reminded of the conditions from which the equations and figures were developed. The conditions included vertical central loading on strip surface footing underlain by a continuous circular cavity together with the range of cavity size, cavity locations, and soil properties stated earlier. While applications may require interpolation within the range of conditions investigated, extrapolation beyond the range should be made with caution.

6 SUMMARY AND CONCLUSIONS

The stability of strip footing overlying a continuous circular cavity was investigated using the upper bound theorem of limit analysis. The collapse footing pressure under vertical central loading was analyzed for a range of cavity size ($W/B=0.5$ to 3.0), cavity location ($D/B=0.5$ to 7.5 , $E/B=0$ to 6.0) and soil properties ($c=23.9$ to 143.6 kN/m², $\phi=5^\circ$ to 35° , $\gamma=15.7$ to 20.4 kN/m³).

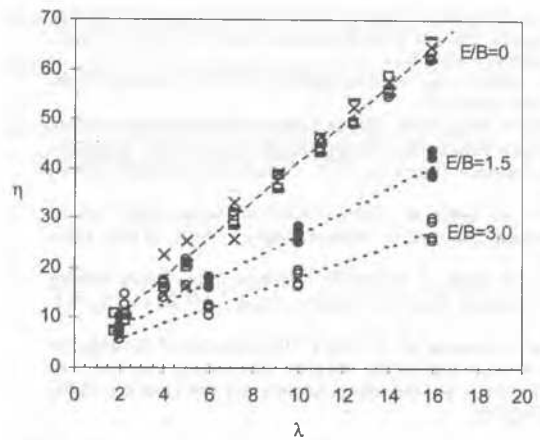


Fig.4 Relation Between η and γ for $E/B=0, 1.5$ and 3.0

From the results of analysis, correlation equations and charts were developed for determination of critical depth to void as well as the ultimate bearing capacity of the footing. Examples were given to demonstrate potential applications of the equations and charts for stability analysis. It is concluded that the results of analysis using the upper bound theorem of limit analysis have provided a database useful for stability analysis of strip footing overlying continuous circular cavities.

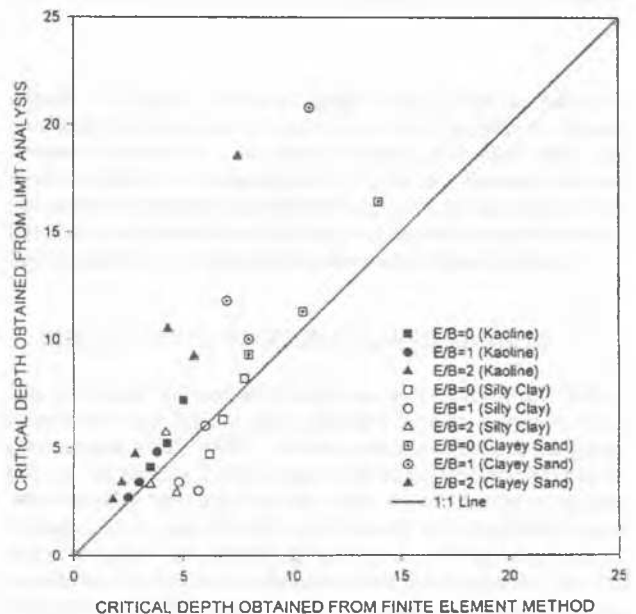


Fig.5 Comparison of Critical Depth Obtained from Limit Analysis and Finite Element Method

7 REFERENCES

- Abdellah, G. A. H. & Abdalla, M. H. (1987). "The Interaction Between a Tunnel/Cavity and Nearby Structures." *Proc. VI Australian Tunneling Conference*, 1, 183-189.
- Badie, A. (1983). "Stability of Spread Footing Supported by Clay Soil with Underground Void." PhD thesis, The Pennsylvania State University, University Park, PA.
- Badie, A. & Wang, M. C. (1984). "Stability of Spread Footing Above Void in Clay." *J. Geotech. Engrg. Div.*, ASCE, 110(11), 1591-1605.
- Badie, A. & Wang, M. C. (1994). "Interaction Between Strip Footing and Soft Ground Tunnel." *Proc., XIII International Conference on Soil Mechanics and Foundation Engineering*, New Delhi, India, 2, 571-574.
- Baus, R. L. (1980). "The Stability of Shallow Continuous Footings Located Above Voids." PhD thesis, The Pennsylvania State University, University Park, PA.

- Baus, R. L. & Wang, M. C. (1983). "The Bearing Capacity of Strip Footing Located Above a Void in Cohesive Soils." *J. Geotech. Engrg. Div.*, ASCE, 109(1), 1-14.
- Chen, W. F. (1974). *Limit Analysis and Soil Plasticity*. Elsevier Scientific, New York, NY.
- Hsieh, C. W. & Wang, M. C. (1992). "Bearing Capacity Determination Method for Strip Surface Footings Underlain by Voids." *Transportation Research Record No. 1336*, Transportation Research Board, 90-95.
- Wang, M. C. & Badie, A. (1985). "Effect of Underground Void on Foundation Stability." *J. Geotech. Engrg.*, ASCE, 111(8), 1008-1019.
- Wang, M. C. & Hsieh, C. W. (1987). "Collapse Load of Strip Footing Above Circular Void." *J. Geotech. Engrg.*, ASCE, 113(5), 511-515.
- Wood, L. A. & Lamach, W. J. (1985). "The Behavior of Footings Located Above Voids." *Proc., Eleventh International Conference on Soil Mechanics and Foundation Engineering*, San Francisco, Calif., 4, 2273-2276.